ACS Catalysis

Research Article

pubs.acs.org/acscatalysis

A Dihydride Mechanism Can Explain the Intriguing Substrate Selectivity of Iron-PNP-Mediated Hydrogenation

Glenn R. Morello and Kathrin H. Hopmann*

Centre for Theoretical and Computational Chemistry and Department of Chemistry, UiT − The Arctic University of Norway, Tromsø N-9037, Norway

Supporting Information

ABSTRACT: Iron-PNP pincer complexes are efficient catalysts for the hydrogenation of aldehydes and ketones. A variety of hydrogenation mechanisms have been proposed for these systems, but there appears to be no clear consensus on a preferred pathway. We have employed high-level quantum chemical calculations to evaluate various mechanistic possibilities for iron-PNP catalysts containing either CH_2, NCH_3, or NH in the PNP linker. For all three catalyst types, we propose that the active species is a *trans*-dihydride complex. For CH_2- and NH-containing complexes, we predict a dihydride mechanism involving a dearomatization of the backbone. The proposed mechanism proceeds through a metal-bound alkoxide intermediate, in excellent agreement with experimental observations. Interestingly, the relative stability of the iron-alkoxide can explain why complexes with NCH_3 in the PNP linker are chemoselective for aldehydes, whereas those with CH_2 or NH in the linker do not show a clear substrate preference. As a general concept in computational catalysis, we recommend to employ known substrate selectivities as a diagnostic factor to evaluate the probability of proposed mechanisms.

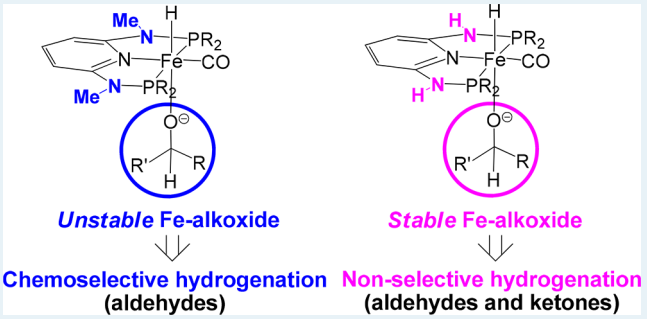

KEYWORDS: *iron-pincer, hydrogenation, chemoselectivity, mechanism, DFT*

INTRODUCTION

The first iron-PNP pincer complexes were reported in the 1970s by Dahlhoff and Nelson.[1,2] Since then, a variety of different iron-PNP complexes have been designed, which have found application in the hydrogenation of alkenes, carbonyl functionalities, and carbon dioxide (for a comprehensive recent review on iron-PNP systems, see ref 2). The groups of Milstein, Hu, and Kirchner have reported different iron-PNP pincer catalysts that can be employed for hydrogenation of ketones and aldehydes.[3−8] The PNP ligands of these catalysts are based on pyridine and diisopropylphosphino moieties, but the atoms connecting these groups are different, with either O, CH_2, NH, or NCH_3 in the linker position (Figure 1).

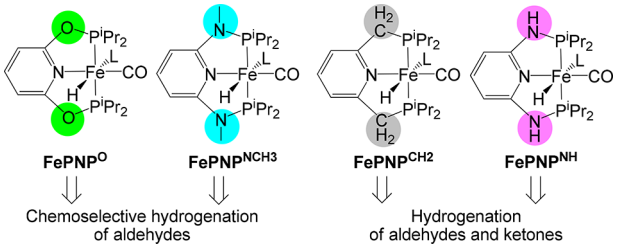

Figure 1. Iron-PNP complexes with O, NCH_3, CH_2, or NH in the ligand linker (L = additional ligand).[3−7]

The mechanisms of iron-PNP pincer complexes have been studied experimentally and computationally, and a number of very different reaction pathways have been proposed. For $FePNP^{CH2}$-mediated ketone hydrogenation, Milstein and co-workers originally suggested a nonredox monohydride mechanism proceeding through dearomatization/aromatization of the PNP ligand,[3] but subsequently the same group proposed a very different outer sphere redox-active dearomatization/aromatization mechanism (Figure 2A).[4] For hydrogenation with $FePNP^{NH}$, Kirchner and co-workers proposed a nonredox monohydride mechanism, which maintains a dearomatized PNP ligand throughout the reaction (Figure 2B).[5] In a comprehensive computational study, Yang was the first to propose an outer-sphere dihydride mechanism for $FePNP^{CH2}$-mediated ketone hydrogenation, in which the PNP-ligand stays aromatized throughout (Figure 2C).[9] On the basis of computations and experimental characterization of putative intermediates, Kirchner and co-workers suggested the same dihydride mechanism for $FePNP^{NCH3}$-mediated aldehyde hydrogenation.[6] The mechanisms proposed for iron-PNP complexes differ widely with respect to the nature of the active species, the oxidation state of the iron center, the coordination

Received: March 9, 2017
Revised: June 28, 2017
Published: July 24, 2017

DOI: 10.1021/acscatal.7b00764
ACS Catal. 2017, 7, 5847−5855

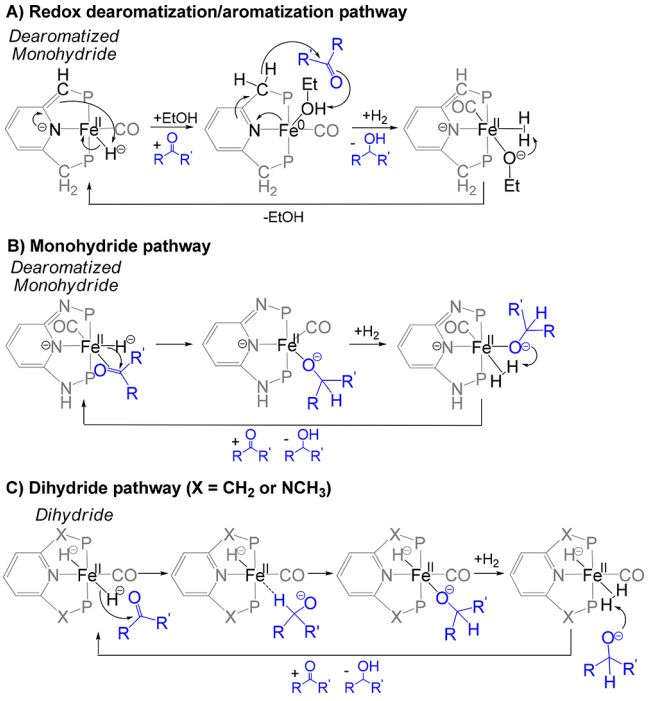

Figure 2. (A) Redox mechanism A proposed by Milstein and co-workers for $FePNP^{CH2}$,[4] (B) monohydride mechanism B proposed by Kirchner and co-workers for $FePNP^{NH}$,[5] and (C) dihydride mechanism C proposed by Yang for $FePNP^{CH2}$,[9] and by Kirchner and co-workers for $FePNP^{NCH3}$[6] (P = P^iPr_2).

of the substrate, and the involvement of the PNP linker in the hydrogenation reaction (Figure 2).

The iron-PNP pincer complexes exhibit different substrate preferences, with $FePNP^{CH2}$ and $FePNP^{NH}$ showing the ability to hydrogenate both ketones and aldehydes,[3−5,8] whereas $FePNP^{NCH3}$ and $FePNP^{O}$ have been reported to be chemoselective for aldehydes.[6,7] It is important to point out that aldehydes intrinsically are more reactive than ketones,[10] which could offer a simple explanation for the preference for aldehydes in $FePNP^{O}$- and $FePNP^{NCH3}$-mediated hydrogenations. This raises the question as to why $FePNP^{NH}$ complexes do not prefer aldehydes as substrates.[5] We propose that the apparent absence of chemoselectivity for $FePNP^{NH}$ is highly intriguing, more so than the presence of chemoselectivity for $FePNP^{NCH3}$.

To understand the substrate selectivity of iron-pincer complexes, it is essential to establish their hydrogenation mechanisms. We have employed state-of-the-art quantum chemical calculations to study the catalysts $FePNP^{NH}$, $FePNP^{NCH3}$, and $FePNP^{CH2}$. The mechanisms proposed in the literature (Figure 2) were compared to new proposals put forward here. Our conclusion is that it is possible to find a clear consensus for iron-pincer-mediated hydrogenation: all three complexes prefer an iron-dihydride complex as the active species. For two of the catalysts, $FePNP^{NH}$ and $FePNP^{CH2}$, we predict a dihydride mechanism involving a dearomatization of the PNP ligand, whereas for $FePNP^{NCH3}$, which cannot undergo dearomatization, an earlier mechanistic proposal is supported (Figure 2C).[6] Both dihydride mechanisms proceed through formation of an iron-alkoxide intermediate. Interestingly, the stability of the iron-alkoxide relative to the iron-dihydride can explain the differences in substrate preferences of iron-PNP hydrogenation catalysts.

COMPUTATIONAL DETAILS

Models. All calculations were performed with full catalysts and substrates (Figure 3), without truncations or symmetry

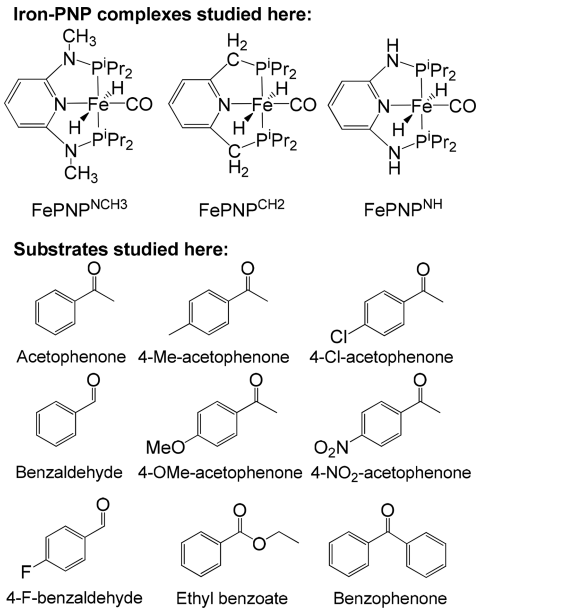

Figure 3. Computational models include full catalyst structures (shown in the dihydride state) and full substrates.

constraints, and with a closed-shell spin state (triplet states were evaluated for the dearomatized species[11]). To model the effect of the experimental solvent, we included the polarizable continuum solvent model IEFPCM (ethanol),[12,13] alongside inclusion of one explicit solvent molecule where relevant, that is, for interaction with an anionic alkoxide intermediate and for binding to the free coordination site in the precatalyst structure. Inclusion of additional solvent molecules was not attempted due to the complications arising from such models.[14] Particular attention was paid to a thorough evaluation of the conformational space, especially the isopropyl groups that can give rise to a number of conformational possibilities. For states that are critical for evaluation of the overall barriers, a minimum of 20 different conformations was evaluated.

Methods. All calculations were performed with *Gaussian 09*, revision D01.[15] Unless explicitly noted otherwise, the DFT functional B3LYP,[16] including both the Grimme empirical dispersion correction (D3[17]) and IEFCPM[18] (ethanol), with the basis set 6-311++G(2d,2p) was employed in geometry optimizations and energy evaluations. Counter poise corrections (CP_{corr}) were computed at the same basis set to estimate the magnitude of the basis set superposition error when joining several molecules into one model.[19,20] The CP_{corr} for combination of the iron-complex with another molecule (H_2, solvent, or substrate) was computed to be 0.2 kcal/mol for H_2, 1.4 kcal/mol for EtOH, and between 1.5 and 2.2. kcal/mol for the nine studied substrates.

For a very small number of transformations, optimization of the transition state (TS) structure in IEFPCM failed. For these systems (marked with an asterisk in the figure and "vacuum" in the Supporting Information), transition states were optimized in vacuum using B3LYP-D3/6-311++G(2d,2p). Single point calculations were subsequently performed on the optimized geometries at the B3LYP-D3/6-311++G(2d,2p)/IEFPCM-

DOI: 10.1021/acscatal.7b00764
ACS Catal. 2017, 7, 5847−5855

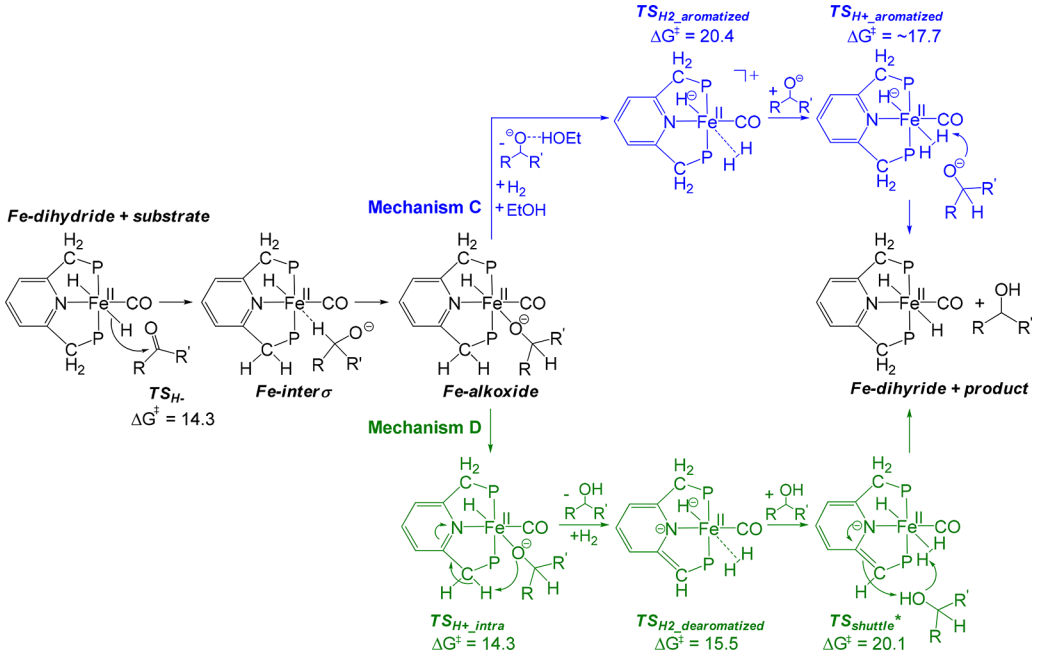

Figure 4. Dihydride mechanism C as proposed by Yang[9] as compared to our alternative proposal, mechanism D, for the substrate acetophenone (P = P^iPr_2). Computed energies relevant to the discussion are shown ($\Delta G_{298K,sol}$, kcal/mol, * = geometry optimized in vacuum; see Computational Details).

(ethanol) level of theory to estimate the solvent effects on the energies.

All stationary states were confirmed through frequency calculations, with only real frequencies for minima and one imaginary frequency for TSs. For selected TSs, the nature of the chemical transformation was confirmed through intrinsic reaction coordinate (IRC) calculations.

Energies. Thermochemical data at 298 K were obtained from frequency calculations at the same level of theory as geometry optimizations. The computed raw Gibbs free energies ($G_{298K,raw}$) correspond to a 1 atm standard state, and to convert them to a solution standard state ($G_{298K,sol}$), a standard state correction was applied.[20] For each separately computed molecule, $G_{298K,sol} = G_{298K,raw} + SS_{Gcorr\_298K}$, where SS_{Gcorr_298K} is the correction to the Gibbs free energy. For each nonsolvent molecule, SS_{Gcorr_298K} equals +1.89 kcal/mol, assuming a 1 M standard state (employing $SS_{Gcorr\_298K} = RT\ \ln[V] = RT\ \ln[RTn/p]$ = 8.31447 J K^{-1} mol^{-1} × 298.15 K × ln[0.08206 L atm K^{-1} mol^{-1} × 298.15 K × 1 mol L^{-1} × 1 atm^{-1}] = +1.89 kcal/mol). For solvent molecules, the standard state of the solvent has to be taken into account.[21] The SS_{Gcorr_298K} for ethanol was estimated as 3.57 kcal/mol, employing the density of ethanol (0.78522 g/cm^3 = >n = 17 mol L^{-1}) in the above equation for SS_{Gcorr_298K}. The solution standard state free energy for each transformation ($\Delta G_{298,sol}$) was obtained as $\Delta G_{298K,sol} = G_{298K,sol}$ (final state) − $G_{298K,sol}$ (initial state) + CP_{corr} (only added if relevant, i.e., if the two states have a different number of molecules).

For reactions with an experimental temperature of 313 K,[6] the *freqcheck* utility was employed to compute the temperature correction (T_{corr}) to the Gibbs free energy. Standard state corrections at 313 K (SS_{Gcorr_313}) equal 2.02 kcal/mol for each nonsolvent molecule and 3.79 kcal/mol for ethanol. For each separately computed molecule, the solution standard state Gibbs free energy at 313 K ($G_{313K,sol}$) was obtained as $G_{313K,sol} = G_{298K,raw} - T_{corr\_298K} + T_{corr\_313K} + SS_{Gcorr\_313K}$.

RESULTS AND DISCUSSION

The $FePNP^{NH}$, $FePNP^{NCH3}$, and $FePNP^{CH2}$ complexes and a set of relevant aldehyde and ketone substrates (Figure 3) were studied using state-of-the art quantum chemical methods to establish energy profiles for different hydrogenation pathways.

For $FePNP^{CH2}$, a variety of mechanisms have been proposed in the literature. We have computed mechanisms A−C as shown in Figure 2, alongside own proposals (vide infra). The redox-active mechanism A involves formation of an aromatized Fe(0) species from a dearomatized Fe(II) monohydride (Figure 2A).[4] We find that the dearomatized iron-monohydride is 12.5 kcal/mol above our energetic reference, the iron-dihydride species (Figure S1). The subsequent formation of the Fe(0) complex has a barrier of 52.5 kcal/mol for direct transfer of a proton from iron to the PNP linker. A TS involving shuttling of the proton through an EtOH molecule, as proposed in an earlier study,[4] could not be located. However, on the basis of earlier results on this system,[4] shuttling of the proton through an EtOH molecule could provide a lowering of the barrier by 15 kcal/mol, which would imply a reduction from 52.5 to 37.5 kcal/mol. Given that the alternative mechanisms evaluated below have overall barriers of ∼20 kcal/mol, mechanism A can be considered unlikely.

Pathway B involves a dearomatized Fe(II) monohydride complex as the active species (Figure 2B). We assume that this species will coordinate an ethanol molecule as a sixth ligand, which has to be replaced by a substrate molecule. The mechanistic steps involving hydride transfer and subsequent proton transfer to a coordinated acetophenone molecule have barriers of 38.0 and 32.9 kcal/mol, respectively, relative to the iron-dihydride complex (Figure S2). This is much higher than other mechanistic alternatives discussed below, making pathway B unlikely.

Pathway C (Figure 2C) involves an iron-dihydride as active species, which transfers a hydride to the free substrate, with a computed barrier of 14.3 kcal/mol for acetophenone (Figure

DOI: 10.1021/acscatal.7b00764
ACS Catal. 2017, 7, 5847−5855

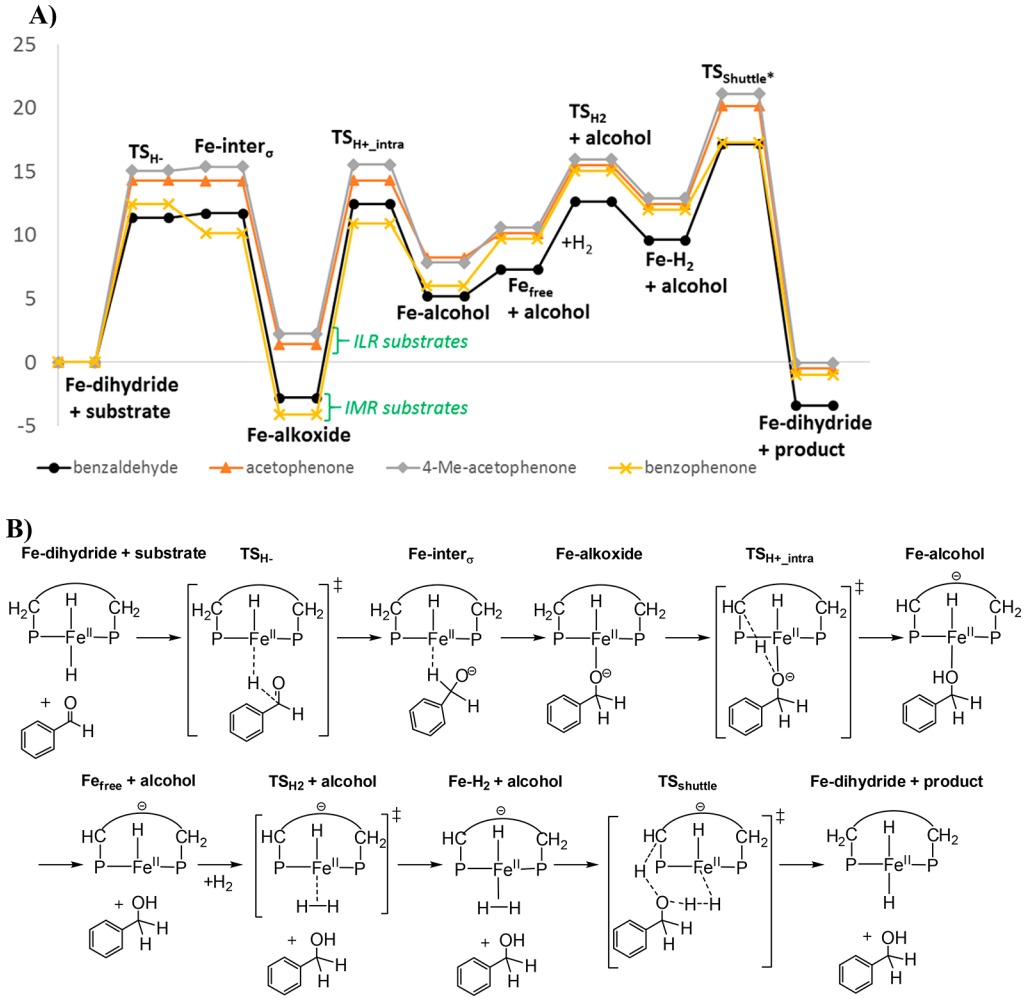

Figure 5. (A) Computed energy profiles ($\Delta G_{298K,sol}$; kcal/mol) for FePNP^{CH2}-mediated hydrogenation of four substrates with mechanism D (* = geometries optimized in vacuum, see Computational Details; IRM = intrinsically more reactive substrates, ILR = intrinsically less reactive substrates). (B) Details of structures given in the energy profile, illustrated with benzaldehyde (catalyst backbone drawn schematically, CO ligand omitted).

4). Initially a C−H σ complex is formed, with the transferred hydrogen loosely coordinated to the iron center. The alkoxide then binds to iron through the oxygen atom to form an iron-alkoxide intermediate. We have evaluated two conceptually different pathways for converting the iron-alkoxide to the alcohol product: The first involves cleavage of the iron-alkoxide bond, and then, as first proposed by Yang,[9] binding of H_2 and heterolytic transfer of a proton to the free alkoxide (pathway C, Figure 4). In this mechanism, the iron complex remains aromatized throughout. For dissociation of the alkoxide (which was solvated with one EtOH molecule to stabilize the negative charge), we compute a cost of 16.2 kcal/mol (Figure S3). Subsequent coordination of H_2 to the iron center has a barrier of 20.4 kcal/mol (Figure 4). An optimized TS for proton transfer from H_2 to the free alkoxide could not be located here, but it is estimated to have a barrier of ~17.7 kcal/mol on the basis of linear transit calculations (results by Yang[9] and our studies on the alternative substrate benzophenone indicate that this proton transfer would not be rate-limiting, Figure S4).

In our conceptually different aromatization/dearomatization pathway D (Figure 4), the iron−alkoxide bond is not broken. Instead an intramolecular proton transfer from the linker-CH_2 to the bound alkoxide occurs, with a barrier of 14.3 kcal/mol. A similar TS has been evaluated by Yang, but was dismissed to be part of the catalytic cycle.[9] Once the neutral product alcohol is formed and released, H_2 coordinates to the dearomatized iron species with a barrier of 15.5 kcal/mol (4.9 kcal/mol below the barrier for H_2 coordination to the aromatized species, Figure 4). A proton can then be transferred from H_2 to the linker to regenerate the aromatized iron-dihydride. Direct proton transfer from H_2 to the linker has a barrier of 28.0 kcal/mol, but shuttling of the proton through an EtOH molecule reduces the barrier to 24.2 kcal/mol, whereas proton shuttling through the formed product alcohol, 1-phenyl-ethanol, has a barrier of only 20.1 kcal/mol (Figure 4, Figure S5; also a stepwise proton transfer was computed, but is not more favorable, Figure S6). To our knowledge, this is the first time the product alcohol has been implicated in the reaction mechanism.

For acetophenone as substrate, the overall barriers for mechanism C and D are 20.4 and 20.1 kcal/mol, respectively (Figure 4). The alternative substrate 4-Me-acetophenone gives barriers of 22.3 and 21.1 kcal/mol, respectively, whereas benzophenone gives barriers of 22.4 and 21.4 kcal/mol, respectively. Although pathway D is preferred for all three substrates, the energy differences are too small to make a definite conclusion. Nonetheless, we suggest that a number of characteristics speak for the aromatization−dearomatization pathway D as the operative mechanism for FePNP^{CH2}-mediated

DOI: 10.1021/acscatal.7b00764
ACS Catal. 2017, 7, 5847−5855

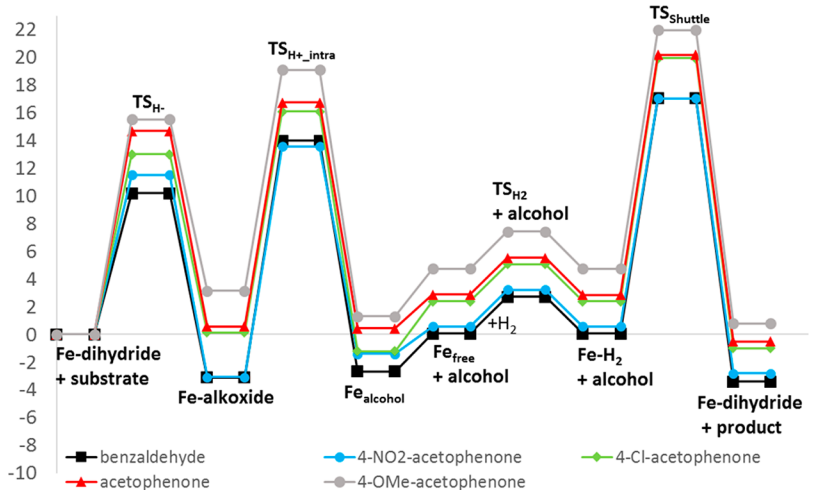

Figure 6. Computed energy profiles ($\Delta G_{298K,sol}$; kcal/mol) for FePNP^{NH}-mediated hydrogenation of five substrates employing mechanism D. For schematic drawing of each state, see Figure 5 (note that the transient Fe-inter$_\sigma$ structure was not computed, as it is not essential for evaluation of the reaction energetics).

hydrogenation: (i) several of the proposed intermediates have been observed in experiments, including the aromatized iron-dihydride and iron-alkoxide,[3] and a dearomatized iron-ethanol complex[4] (a dearomatized species should not be observed in mechanism C), (ii) for the three evaluated ketones, cleavage of the iron−alkoxide bond (mechanism C, Figures S3 and S4) has a 2−3 kcal/mol higher cost than the barrier for intramolecular proton transfer to form the bound neutral alcohol (mechanism D, TS$_{H+_intra}$, Figure 5), making the latter more likely, and (iii) for the three evaluated ketones, H_2 coordination to the dearomatized complex (mechanism D) has a 3−6 kcal/mol lower barrier than H_2 coordination to the aromatized species (mechanism C, Figure 4), implying that dearomatization promotes H_2 binding.

We proceeded to compare experimental and theoretical results for FePNP^{CH2}-mediated hydrogenation of four substrates, assuming mechanism D is operative (Figure 5). If the computed intrinsic hydride affinity of each substrate is taken as a measure for its reactivity, then acetophenone and 4-Me-acetophenone are expected to be intrinsically less reactive than benzophenone and benzaldehyde (Table S2 and Figure S7). However, in contrast to this expectation, in experiments, acetophenone shows slightly higher conversion than benzophenone (also higher than benzaldehyde, however, this substrate shows conflicting results; see ref 22).[3,4] For the substrates benzophenone and 4-Me-acetophenone, the computed intrinsic hydride affinity differs by 3.9 kcal/mol (Table S2), but in experiments, FePNP^{CH2}-mediated hydrogenation of these two substrates leads to only small yield differences.[4] Remarkably, mechanism D is able to provide an explanation for the experimentally observed substrate preferences of FePNP^{CH2}. As shown in Figure 5, the intrinsically more reactive substrates benzophenone and benzaldehyde lead to formation of energetically low-lying iron-alkoxides (below the iron-dihydride), whereas the intrinsically less reactive substrates acetophenone and 4-Me-acetophenone do not. An effect of this is that the overall hydrogenation barriers of the intrinsically more reactive substrates are raised, making them similar to that of the less reactive substrates. Although benzophenone initially is more reactive (the hydride transfer barrier is below that of 4-Me-acetophenone, Figure 5), the iron-alkoxide formed from benzophenone is far more stable, making the final barriers for these two substrates similar. With temperature corrections (313 K), the overall hydrogenation barriers are 21.6 kcal/mol for benzophenone and 22.1 kcal/mol for 4-Me-acetophenone, in excellent agreement with the reported small experimental yield differences (Table S2).[4]

It should be noted that a previous study concluded that it is unlikely that an iron-dihydride is involved in FePNP^{CH2}-mediated hydrogenations, because this species "did not show any significant reactivity towards acetophenone (after one day)".[4] It is unclear how this experiment was performed and if, for example, H_2 was added. In our calculations, the reaction of acetophenone with the iron-dihydride to form the alkoxide species is endothermic (Figure 5), which might explain the absence of activity. When H_2 is added, our computations indicate a small driving force toward formation of 1-phenyl-ethanol (Figure 5). It would be recommended to test the activity of the iron-dihydride with other substrates, for example, benzophenone, to evaluate if an iron-alkoxide is formed.

We proceeded to evaluate mechanistic alternatives for the related pincer complex, FePNP^{NH} (Figure 1). For this complex, the nonredox dearomatization/aromatization mechanism B has been proposed (Figure 2B). We find that for hydrogenation of acetophenone, the overall barrier for pathway B is 32.7 kcal/mol (Figure S8). If we instead assume that the dihydride mechanism D (Figure 4) is operative, we find an overall barrier of 20.2 kcal/mol for acetophenone, making this a more likely path. Similar to FePNP^{CH2}, H_2 coordination to the dearomatized species of FePNP^{NH} is lower in energy than H_2 coordination to the aromatized species (in this case by 12.5 kcal/mol), which speaks for pathway D as the operative mechanism also for FePNP^{NH} (however, we cannot exclude pathway C as potentially operative, Figure S9). For regeneration of the active species in pathway D, we find that direct proton transfer from H_2 to the linker is costly (33.2 kcal/mol), in agreement with earlier results by Kirchner and co-workers (although for a related complex, a direct transfer was considered feasible[23]).[5] However, shuttling of the proton through EtOH reduces the barrier to 22.5 kcal/mol, and shuttling through 1-phenyl-ethanol lowers it to 20.2 kcal/mol, making mechanism D a feasible pathway for FePNP^{NH}, as for FePNP^{CH2}. For FePNP^{NH}, shuttling through 1-phenyl-ethanol versus ethanol was also evaluated with a larger molecular model

DOI: 10.1021/acscatal.7b00764
ACS Catal. 2017, 7, 5847−5855

Table 1. Comparison of Computed Barrier Differences ($\Delta\Delta G^{\ddagger}$, kcal/mol) to Approximated Experimental Values for $FePNP^{CH2}$-, $FePNP^{NH}$-, and $FePNP^{NH3}$-Mediated Hydrogenation of Different Substrates

complex and mechanism	substrate	overall barrier $\Delta G^{\ddagger}_{computed}$	$\Delta\Delta G^{\ddagger}_{computed}$ [b]	$\Delta\Delta G^{\ddagger}_{experiment}$ [c] (approximation)	error $\Delta\Delta G^{\ddagger}$ [d]
Mechanisms Proposed Here					
$FePNP^{CH2}$, mechanism D[a,e]	acetophenone	21.1			
	benzophenone	21.6	+0.5	+0.1	+0.4
	4-Me-acetophenone	22.1	+1.0	+0.3	+0.7
$FePNP^{NH}$, mechanism D[e]	acetophenone	20.2			
	benzaldehyde	20.1	−0.1	+0.9	−0.9
	4-NO_2-acetophenone	20.1	−0.1	+0.4	−0.5
	4-Cl-acetophenone	21.2	+1.0	+0.0	+1.0
	4-OMe-acetophenone	22.0	+1.8	+0.6	+1.2
$FePNP^{NCH3}$, mechanism C[f]	4-F-benzaldehyde	18.0			
	acetophenone	22.0	+4.0	≥ +2.9	≥0.0
	ethyl benzoate	28.6	+10.5	≥ +2.9	≥0.0
Earlier Mechanistic Proposal					
$FePNP^{NH}$, mechanism B[g]	acetophenone	32.7			
	4-NO_2-acetophenone	47.1	+14.4	+0.4	+14.0

[a]Benzaldehyde is not included due to conflicting results.[22] [b]Barrier difference between given substrate and reference substrate (reference substrate: acetophenone for $FePNP^{CH2}$ and $FePNP^{NH}$, and 4-F-benzaldehyde for $FePNP^{NCH3}$). T = 298 K for $FePNP^{NH}$ and 313 K for $FePNP^{CH2}$ and $FePNP^{NCH3}$. [c]Experimental yields[4−6] were converted to rough approximate barrier differences (Table S3). [d]$\Delta\Delta G^{\ddagger}_{computed} - \Delta\Delta G^{\ddagger}_{experiment}$. [e]Figures 5 and 6. [f]Figure 7. [g]Figure 2B.[5]

(Table S1), which reproduced the preference for 1-phenylethanol.

$FePNP^{NH}$ hydrogenates both ketones and aldehydes in experiments.[5] For five known substrates, we have computed the intrinsic hydride affinities, which indicate that 4-NO_2-acetophenone should be the most reactive substrate, followed by benzaldehyde, 4-Cl-acetophenone, acetophenone, and 4-OMe-acetophenone (Table S2). However, in experiments, acetophenone hydrogenation is preferred, whereas 4-NO_2-acetophenone and 4-OMe-acetophenone, which have a hydride affinity difference of 7.4 kcal/mol (Table S2), unexpectedly provide similar yields.[5] If we assume that mechanism D is operative for $FePNP^{NH}$, we obtain results similar to those for $FePNP^{CH2}$: the iron-alkoxides formed from the intrinsically more reactive substrates are low in energy, which raises their overall barriers (Figure 6), making these similar to the intrinsically less reactive substrates. Thus, the formation of stable iron-alkoxides from the reactive substrates is able to explain why $FePNP^{NH}$ does not appear to show a preference for aldehydes (or activated ketones).

To quantitatively compare our results to experiment,[4,5] we have converted experimental yields into approximate barrier differences relative to acetophenone ($\Delta\Delta G^{\ddagger}_{experiment}$, Table S3), and have compared these to computed values for $FePNP^{CH2}$ and $FePNP^{NH}$ (Table 1). We emphasize that the experimental barrier differences should be considered rough estimates, but it can be noted that absolute errors relative to computed $\Delta\Delta G^{\ddagger}$ values are small, 0.4−1.2 kcal/mol (Table 1). This supports that mechanism D is operative for $FePNP^{CH2}$ and $FePNP^{NH}$. We have also evaluated a barrier difference assuming that $FePNP^{NH}$ employs the earlier proposed mechanism B (Figure 2).[6] The predicted hydrogenation barrier for 4-NO_2-acetophenone becomes as high as 47.1 kcal/mol, which is 14.4 kcal/mol above the barrier for acetophenone. This is in strong disagreement with the fact that both substrates are converted in experiment,[5] with an experimental barrier difference approximated here to 0.4 kcal/mol (Table 1). The high barriers and the high barrier difference for these two substrates indicate that mechanism B is not operative for $FePNP^{NH}$.

Finally, we turned to the iron pincer-complex $FePNP^{NCH3}$, which cannot undergo deprotonation of the PNP linker. For this complex, Kirchner and co-workers have proposed mechanism C to be operative.[6] We have tested different pathways with the substrate benzaldehyde (mechanism B, Figure S10, mechanism C, Figure S11, and an alternative proposed here, mechanism E, Figure S12) and find that mechanism C indeed appears to be preferred for $FePNP^{NCH3}$-mediated hydrogenation. This mechanism involves formation of an iron-alkoxide, followed by cleavage of the iron-alkoxide bond, coordination of H_2, and alkoxide-mediated heterolytic cleavage of H_2 (Figure 7).

In experiments, $FePNP^{NCH3}$ is chemoselective for aldehydes and appears unable to hydrogenate ketones and various other functional groups (in competition experiments with 4-F-benzaldehyde, >99% product originated from the aldehyde and <1% from a ketone or an ester).[6] The experimental values indicate that the barrier differences ($\Delta\Delta G^{\ddagger}$) between aldehyde and the other substrates are ≥ +2.9 kcal/mol (Table S3). We have here compared $FePNP^{NCH3}$-mediated hydrogenation of 4-F-benzaldehyde, acetophenone, and ethyl benzoate with mechanism C and obtain barriers of 18.0, 22.0, and 28.6 kcal/mol, respectively (Figure 7), in excellent agreement with experiment (Table 1). Interestingly, in contrast to $FePNP^{CH2}$ and $FePNP^{NH}$, the iron-alkoxide intermediate formed from $FePNP^{NCH3}$ and 4-F-benzaldehyde is not energetically low-lying,[24] implying that the hydrogenation barrier remains low, preserving the intrinsically higher reactivity of the aldehyde.

On the basis of the results obtained for the three studied pincer complexes, we propose that the stability of the iron-alkoxide relative to the iron-dihydride is the decisive factor determining the substrate selectivity of iron-pincer-mediated hydrogenation reactions. If a given complex forms unstable iron-alkoxides (as is the case for $FePNP^{NCH3}$), the substrate selectivity is governed by the intrinsic substrate properties, implying that aldehydes (or activated ketones) are the preferred substrates. If the complex forms stable iron-alkoxides from reactive substrates (as is the case for $FePNP^{NH}$ and $FePNP^{CH2}$), the barrier of the intrinsically more reactive substrates

DOI: 10.1021/acscatal.7b00764
ACS Catal. 2017, 7, 5847−5855

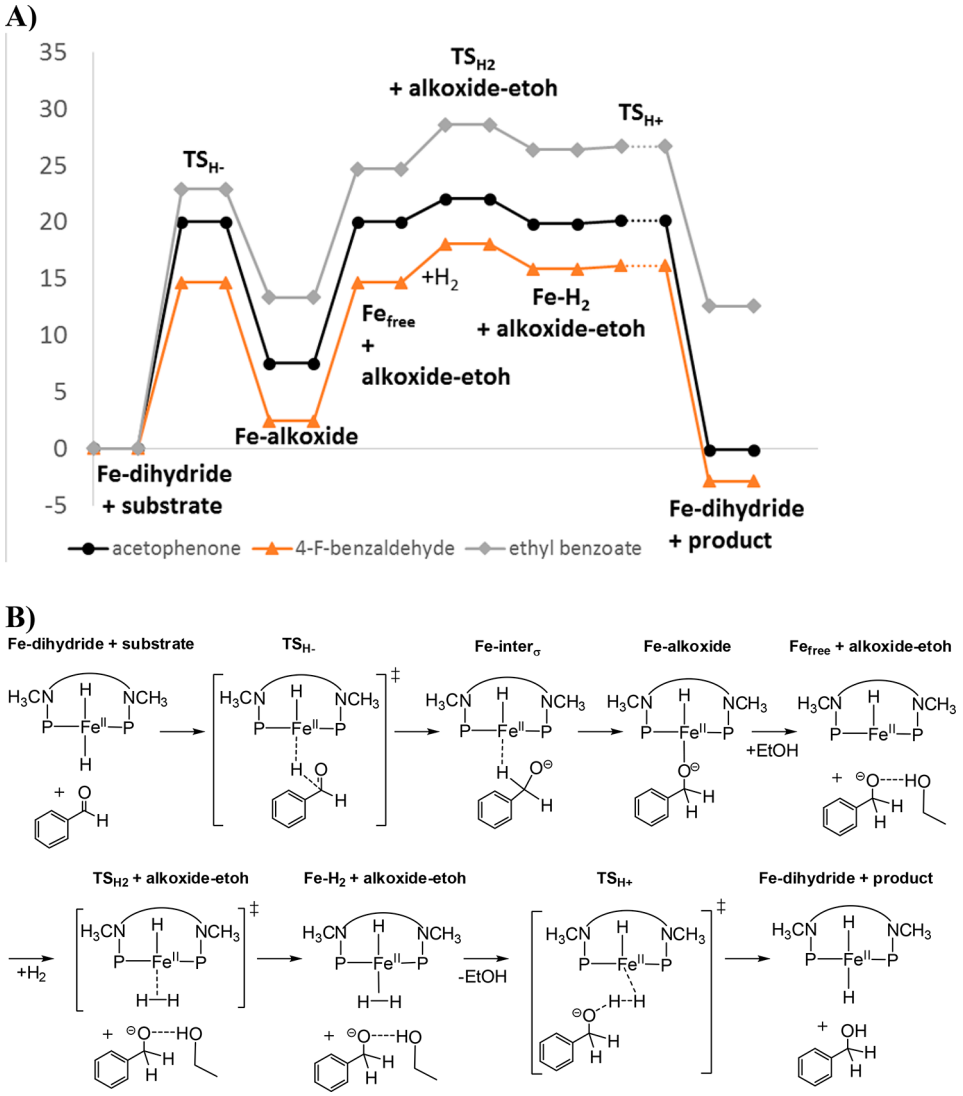

Figure 7. (A) Computed energy profiles ($\Delta G_{313K,sol}$; kcal/mol) for FePNP^{NCH3}-mediated hydrogenation of three substrates employing mechanism C. TS$_{H+}$ could not be fully optimized, and the given energies are estimated. Results by Gorgas et al. indicate that TS$_{H+}$ is not rate-limiting.[6] (B) Details of the computed structures, illustrated with benzaldehyde (catalyst drawn simplified, CO ligand omitted). The transient intermediate Fe-inter$_\sigma$ is not essential to the evaluation of the energetics and was not computed.

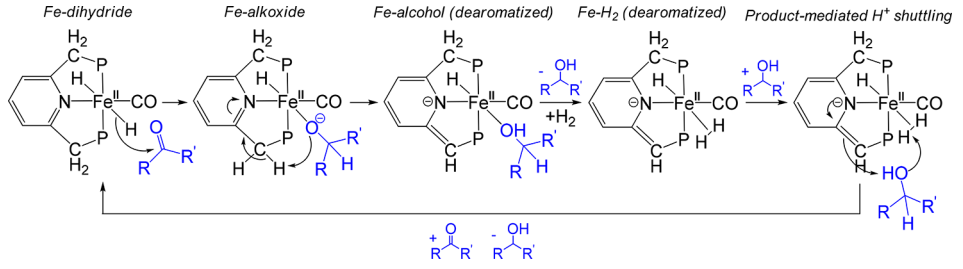

Figure 8. Dihydride aromatization/dearomatization pathway D proposed here for FePNP^{CH2}- and FePNP^{NH}-mediated hydrogenation of aldehydes and ketones (P = P^{i}Pr$_2$, a transient σ intermediate formed prior to the Fe-alkoxide state is not shown here; see Figure 5, Fe-inter$_\sigma$).

(aldehydes or activated ketones) is raised, so that the experimental yields become similar to those of less reactive substrates (such as acetophenone). Although FePNP^{NH} and FePNP^{CH2} thus appear nonselective, in excellent agreement with experimental results,[3−5] one can speculate that under conditions where a substrate exhibits two functionalities, for example, an aldehyde and a ketone group, FePNP^{NH} and FePNP^{CH2} would first react with the aldehyde to form a low-lying alkoxide, which would effectively raise the barrier for ketone hydrogenation, reducing hydrogenation of the later.[25] Currently, we are extending our study to include the hydrogenation mechanism and selectivity of FePNP^{O}, to evaluate if this complex also follows the trend expected on the basis of the results put forward here for FePNP^{CH2}, FePNP^{NH}, and FePNP^{NCH3}.[26]

DOI: 10.1021/acscatal.7b00764
ACS Catal. 2017, 7, 5847−5855

CONCLUSIONS

We have evaluated the hydrogenation mechanisms of the iron-pincer complexes $FePNP^{CH2}$, $FePNP^{NH}$, and $FePNP^{NH3}$, and we propose that all three catalysts employ a dihydride as active species, in contrast to several earlier mechanistic proposals.[3−5] Interestingly, the dihydride mechanisms proposed here are able to explain the substrate selectivity of all three iron-pincer complexes.

For $FePNP^{CH2}$- and $FePNP^{NH}$-mediated hydrogenation, we predict reaction pathway D involving hydride transfer to the free substrate, formation of an iron-alkoxide intermediate, intramolecular proton transfer from the PNP linker to the alkoxide, alcohol release, H_2 coordination to the dearomatized species, and product-mediated proton-shuttling to the PNP linker, which regenerates the active dihydride species and is rate-limiting (Figure 8). The first step of this mechanism is as originally proposed by Yang (Figure 2C),[9] but the following steps are different from earlier proposals. A number of characteristics speak for mechanism D as the operative mechanism: (i) several of the proposed intermediates have been observed in experiments, including the iron-dihydride,[3,5] an iron-alkoxide,[3,5] and a dearomatized iron-alcohol species,[4] (ii) intramolecular proton transfer from the PNP linker to the bound alkoxide to form the bound neutral alcohol product is preferred over cleavage of the alkoxide−iron bond and release of a charged species, and (iii) for both $FePNP^{CH2}$ and $FePNP^{NH}$, H_2 coordination to the dearomatized iron species has a significantly lower barrier (up to 12.5 kcal/mol) than the barrier for H_2 coordination to the aromatized species. This indicates that formation of the dearomatized complex is advantageous for H_2 binding. Comparison of the experimental yields to computed relative barrier differences for eight $FePNP^{CH2}$- and $FePNP^{NH}$-mediated hydrogenation reactions strongly supports the proposed mechanism D (Table 1). In light of the results obtained here, future experimental studies on the reaction intermediates of $Fe(PNP^{CH2})$ and $Fe(PNP^{NH})$ complexes are desirable.

For $FePNP^{NCH3}$, our calculations support the dihydride mechanism proposed by Kirchner and co-workers, based on the original proposal by Yang.[6,9] This mechanism proceeds through hydride transfer to the free substrate, cleavage of the iron-alkoxide bond, coordination of H_2, and alkoxide-mediated H_2 cleavage (Figure 2, mechanism C). This mechanism correctly predicts aldehydes to be the preferred substrates in $FePNP^{NCH3}$-catalyzed hydrogenation reactions (Table 1).

Both mechanism D (proposed here for $FePNP^{NH}$ and $FePNP^{CH2}$) and mechanism C (proposed for $FePNP^{NCH3}$) proceed through formation of an iron-alkoxide intermediate. This iron-alkoxide has earlier been dismissed in computations on $FePNP^{CH2}$, because its formation would result in an increase of the hydrogenation barrier.[4] Here, we wish to raise the following points: (i) the low energy of the iron-alkoxide intermediate and the low barrier for its formation make it very likely that this intermediate will be formed, (ii) iron-alkoxides have been observed in experiments for $FePNP^{CH2}$ and $FePNP^{NH3}$,[3,6] supporting formation of such a species, and (iii) hydrogenation can be energetically feasible also with an iron-alkoxide formed, as shown here. Interestingly, the formed iron-alkoxide can explain experimentally observed substrate preferences. On the basis of our results, we propose that the stability of the formed iron-alkoxide relative to the iron-dihydride constitutes the main selectivity-determining factor in iron-pincer-mediated hydrogenation reactions. $FePNP^{NCH3}$ forms unstable iron-alkoxides (Figure 7), implying that the intrinsically higher reactivity of aldehydes is preserved, explaining the chemoselectivity observed in experiments.[6] $FePNP^{NH}$ and $FePNP^{CH2}$ convert the intrinsically more reactive substrates (aldehydes and activated ketones) into energetically low-lying, stable iron-alkoxides (Figures 5 and 6), implying that the hydrogenation barriers for these substrates are raised and become similar to those of less reactive substrates, thereby eradicating any intrinsically expected substrate preferences, in excellent agreement with experiment.[3−5]

Our conclusions are based on state-of-the-art DFT calculations, including full molecular structures without truncations, dispersion corrections, a PCM solvent model, and, where relevant, explicit solvation with an ethanol molecule. It can be noted though that any computational model is only an approximation of the real experimental system, and it is possible that effects related to solvation or concentration are not adequately captured. For the type of computational protocol employed here, the error on absolute energies can be several kcal/mol;[13] however, relative energies, such as barrier differences between two substrates, are likely to be more accurate. We have compared the relative activities of three iron-pincer complexes with nine substrates, and see very good agreement with experimental trends, indicating that our computational model is able to capture the differences between the studied systems.

We further emphasize that the selectivity of a system can give important clues about the reaction mechanism and should not be overlooked in computational studies. The mechanisms proposed here correlate well with the experimental substrate preferences of the different iron-PNP complexes, but we have shown that this is not the case for an earlier mechanistic proposal (Table 1). As a general concept in computational catalysis, we recommend to employ known substrate preferences as a diagnostic factor to evaluate the probability of proposed mechanisms.

ASSOCIATED CONTENT

Supporting Information

The Supporting Information is available free of charge on the ACS Publications website at DOI: 10.1021/acscatal.7b00764.

Details of alternative reaction pathways, computed hydride affinities, and conversion of experimental yields into approximate $\Delta\Delta G^{\ddagger}$ values (PDF)

File with optimized coordinates, free energies, and imaginary frequencies; the file with all structures can be conveniently visualized with the Mercury program from the Cambridge Crystallographic Data Centre (XYZ)

AUTHOR INFORMATION

Corresponding Author

*E-mail: kathrin.hopmann@uit.no.

ORCID

Kathrin H. Hopmann: 0000-0003-2798-716X

Notes

The authors declare no competing financial interest.

DOI: 10.1021/acscatal.7b00764
ACS Catal. 2017, 7, 5847−5855

■ ACKNOWLEDGMENTS

This work has been supported by the Research Council of Norway through a FRINATEK grant (no. 231706) and a Centre of Excellence Grant (no. 179568), by the Tromsø research foundation (no. TFS2016KHH), and by Notur - The Norwegian Metacenter for Computational Science through grants of computer time (nos. nn9330k and nn4654k).

■ REFERENCES

(1) Dahlhoff, W. V.; Nelson, S. M. *J. Chem. Soc. A* **1971**, 2184−2190.
(2) Bauer, G.; Hu, X. *Inorg. Chem. Front.* **2016**, *3*, 741−765.
(3) Langer, R.; Leitus, G.; Ben-David, Y.; Milstein, D. *Angew. Chem., Int. Ed.* **2011**, *50*, 2120−2124.
(4) Langer, R.; Iron, M. A.; Konstantinovski, L.; Diskin-Posner, Y.; Leitus, G.; Ben-David, Y.; Milstein, D. *Chem. - Eur. J.* **2012**, *18*, 7196−7209.
(5) Gorgas, N.; Stöger, B.; Veiros, L. F.; Pittenauer, E.; Allmaier, G. N.; Kirchner, K. *Organometallics* **2014**, *33*, 6905−6914.
(6) Gorgas, N.; Stöger, B.; Veiros, L. F.; Kirchner, K. *ACS Catal.* **2016**, *6*, 2664−2672.
(7) Mazza, S.; Scopelliti, R.; Hu, X. *Organometallics* **2015**, *34*, 1538−1545.
(8) Zell, T.; Ben-David, Y.; Milstein, D. *Catal. Sci. Technol.* **2015**, *5*, 822−826.
(9) Yang, X. *Inorg. Chem.* **2011**, *50*, 12836−12843.
(10) Clayden, J.; Greeves, N.; Warren, S.; Wothers, P. *Organic Chemistry*; Oxford University Press: New York, 2001; p 616.
(11) We have evaluated the triplet state of the dearomatized $FePNP^{CH2}$ species Fe_{free}, Figure 5. The geometry optimized triplet state is almost trigonal bipyramidal (in contrast to the square-pyramidal singlet) and has a Gibbs free energy of 5.3 kcal/mol above the singlet, making its involvement during the catalytic steps unlikely.
(12) In a recent benchmark study on iridium-mediated reactions, we found that this solvent model performs very well, see ref 13.
(13) Hopmann, K. H. *Organometallics* **2016**, *35*, 3795−3807.
(14) Inclusion of additional weakly interacting solvent molecules was not attempted, as they would have a large degree of conformational freedom, making it difficult to converge structures and, in particular, to establish the energetically preferred conformation in each case. Variations in the interactions (between solvent molecules, and between solvent and the remaining model) can also severely affect energetics, which would make a comparison of the energies of different states (e.g., reactant and TS) inadequate.
(15) Frisch, M. J.; Trucks, G. W.; Schlegel, H. B.; Scuseria, G. E.; Robb, M. A.; Cheeseman, J. R.; Scalmani, G.; Barone, V.; Mennucci, B.; Petersson, G. A.; Nakatsuji, H.; Caricato, M.; Li, X.; Hratchian, H. P.; Izmaylov, A. F.; Bloino, J.; Zheng, G.; Sonnenberg, J. L.; Hada, M.; Ehara, M.; Toyota, K.; Fukuda, R.; Hasegawa, J.; Ishida, M.; Nakajima, T.; Honda, Y.; Kitao, O.; Nakai, H.; Vreven, T.; Montgomery, J. A., Jr.; Peralta, J. E.; Ogliaro, F.; Bearpark, M.; Heyd, J. J.; Brothers, E.; Kudin, K. N.; Staroverov, V. N.; Kobayashi, R.; Normand, J.; Raghavachari, K.; Rendell, A.; Burant, J. C.; Iyengar, S. S.; Tomasi, J.; Cossi, M.; Rega, N.; Millam, J. M.; Klene, M.; Knox, J. E.; Cross, J. B.; Bakken, V.; Adamo, C.; Jaramillo, J.; Gomperts, R.; Stratmann, R. E.; Yazyev, O.; Austin, A. J.; Cammi, R.; Pomelli, C.; Ochterski, J. W.; Martin, R. L.; Morokuma, K.; Zakrzewski, V. G.; Voth, G. A.; Salvador, P.; Dannenberg, J. J.; Dapprich, S.; Daniels, A. D.; Farkas, Ö.; Foresman, J. B.; Ortiz, J. V.; Cioslowski, J.; Fox, D. J. *Gaussian 09*, revision D.01; Gaussian, Inc.: Wallingford, CT, 2009.
(16) (a) Becke, A. D. *Phys. Rev. A: At., Mol., Opt. Phys.* **1988**, *38*, 3098−3100. (b) Lee, C.; Yang, W.; Parr, R. G. *Phys. Rev. B: Condens. Matter Mater. Phys.* **1988**, *37*, 785−789.
(17) Grimme, S.; Antony, J.; Ehrlich, S.; Krieg, H. *J. Chem. Phys.* **2010**, *132*, 154104.
(18) (a) Tomasi, J.; Mennucci, B.; Cammi, R. *Chem. Rev.* **2005**, *105*, 2999−3093. (b) Tomasi, J.; Mennucci, B.; Cancès, E. *J. Mol. Struct.: THEOCHEM* **1999**, *464*, 211−216. (c) Cancès, E.; Mennucci, B.; Tomasi, J. *J. Chem. Phys.* **1997**, *107*, 3032−3041.
(19) (a) Boys, S. F.; Bernardi, F. *Mol. Phys.* **1970**, *19*, 553−566. (b) Simon, S.; Duran, M.; Dannenberg, J. J. *J. Chem. Phys.* **1996**, *105*, 11024−31.
(20) Cramer, C. J. *Essentials of Computational Chemistry: Theories and Models*; John Wiley & Sons Ltd.: New York, 2002; p 183.
(21) Sparta, M.; Riplinger, C.; Neese, F. *J. Chem. Theory Comput.* **2014**, *10*, 1099−1108.
(22) Benzaldehyde shows low conversion with $FePNP^{CH2}$,[3,4] which has been attributed to formation of benzoic acid through a Cannizzaro reaction.[3,8] Benzoic acid might inactivate the catalyst,[3] but it is unclear how. With acetophenone or trietanolamine as additive, benzaldehyde can be hydrogenated.[3,8] Under the later conditions, conversion of benzaldehyde with an iron-PNP dihydride (P = P^tBu_2) is low (8%);[8] however, the bulky ^{t}Bu groups might inhibit the activity.
(23) Bichler, B.; Holzhacker, C.; Stöger, B.; Puchberger, M.; Veiros, L. F.; Kirchner, K. *Organometallics* **2013**, *32*, 4114−4121.
(24) A previous study on $FePNP^{NCH3}$ appears contrasting, reporting a low-lying iron-alkoxide, 9.3 kcal/mol below the iron-dihydride.[6] However, the previous study employed the simplified substrate acetaldehyde and an iron-dihydride geometry that is 5 kcal/mol higher in energy than the structure found here (Figure S13). This results in an overestimation of the iron-alkoxide stability.
(25) This might explain results observed for $FePNP^{CH2}$, where mixing of benzaldehyde and acetophenone leads to, respectively, 85% and 6% yield of the corresponding alcohols (see Supporting Information of ref 3).
(26) Morello, G.; Hopmann, K. H., manuscript in preparation.

DOI: 10.1021/acscatal.7b00764
ACS Catal. 2017, 7, 5847−5855